Predictive Numerical Simulation of Lamb Wave Scattering from a Wing Skin Defect for Structural Health Monitoring System Design

N. RAJIC[1], C. ROSALIE[1], W. ONG[2] and W. K. CHIU[2]

ABSTRACT

This paper reports on an investigation into the accuracy of numerical finite element simulations of elastic wave scattering from a structural defect in a metallic wing skin component. The work forms part of a broader research program that seeks to develop a validated predictive modelling capability for optimal design of acousto-ultrasonic systems for health monitoring of structural hot spots. The present investigation examines the efficacy of simplified representations of the acoustic transduction process whereby piezoelectric coupling is replaced by a set of traction forces with appropriate time modulation. The motivation for the work is the prospect of a significant gain in computational efficiency. Several different approximation schemes are considered and assessed on the basis of how closely the resulting simulations match experimental observations of the scattered field. Some of the approximation schemes are shown to produce simulation results with an accuracy comparable to that of a piezoelectrically coupled solution, suggesting that improved computational efficiency can be achieved without compromising simulation accuracy.

1. INTRODUCTION

The diagnostic capabilities of acousto-ultrasonic (AU) in-situ structural health monitoring (SHM) methods derive from the detection of scattering of incident waves by structural defects. An accurate prediction of the scattered field is therefore an important requirement for the design of an effective AU system. In the aerospace context, structural wave guides account for the majority of potential SHM applications. For this class of problem the scattering from a defect is influenced by factors such as dispersive wave propagation, the modal composition of the incident wave field, and structural irregularities in the wave guide due, for example, to the presence of fastened assemblies, integral stiffeners, and variations in section thickness; all relatively common features in modern aircraft construction. An optimal SHM strategy would need to account for at least some of these factors, which makes the design problem particularly challenging.

At present, the most reliable approach to the design of an SHM system is empirical. That is, design objectives such as the required number and location of piezoceramic transducers, and the optimal wavenumber and frequency bandwidth for interrogation are in general most reliably determined through an experimental test program [1]. However, the approach needs to balance two competing factors. On the one hand the number of design parameters to consider is large while on the other practical resource constraints limit the scope of experimental investigations. Consequently, the potential for a compromised design outcome is high.

In principle, numerical modelling offers a far more efficient, effective and practical basis for design. For example, the finite element method (FEM) provides a relatively straightforward means of simulating the elastic wave dynamics in structural components and is sufficiently flexible to accommodate an almost arbitrary level of problem complexity. However, the risk of inaccuracy in a numerical simulation generally increases as the complexity of the dynamic modelling problem grows. Two of the most significant contributing factors are: (i) geometric complexity in the structure, and (ii) the transduction characteristics of the acoustic source, which is typically an adhesively-bonded piezoceramic element.

Such factors can be handled by a multi-physics FEM analysis, and given a careful modelling approach the prospect for useful predictive accuracy is reasonable. However, the computational expense of a simulation is generally high even for a moderate level of structural complexity. One particularly burdensome inefficiency relates to the use of implicit integration to temporally advance solutions involving elasto-electromagnetic coupling. Implicit integration is necessary to solve for the coupled fields in the piezoelectric component of the model, but the scheme is neither necessary nor efficient in propagating an elastic

disturbance through a non-piezoelectric material, i.e. the structural host. Interestingly, the finite-difference time-domain method allows for the coupled and uncoupled parts of the problem to be advanced using separate schemes, which leads to comparatively much faster solutions for such problems [2]. However, the difficulties in adapting a finite difference method to irregular structural geometries can often outweigh the computational speed advantage for problems involving real structural components, leaving FEM as the preferred approach.

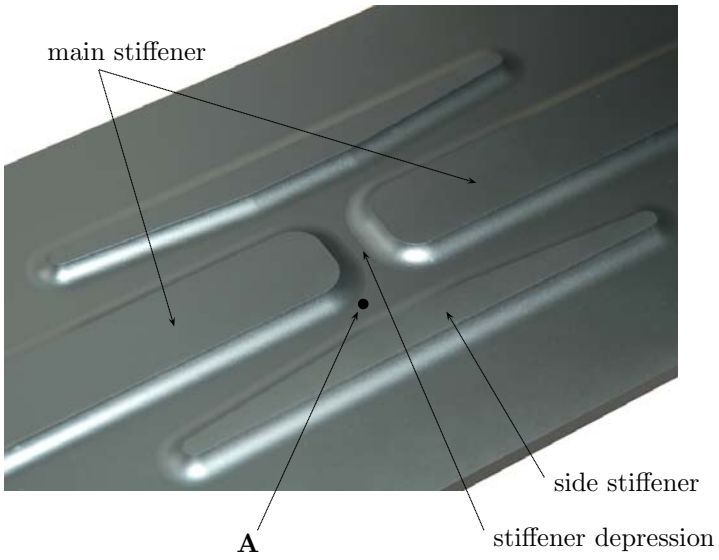

Figure 1. Interior structural detail in the F-111C lower wing skin. The point marked **A** identifies the approximate location of the piezoelectric source transducer (which is bonded to the external side of the wing skin).

In theory, piezoelectric coupling can be eliminated from an FEM simulation by replacing the process of electromechanical transduction with an equivalent set of traction forces. The potential gain in computational efficiency is significant, however the approach is not straightforward as these forces stem from a phenomenon in which a large number of elastic, electric and piezoelectric material constants have a role [2] and furthermore the transfer of those forces is strongly influenced by the properties of the adhesive bondline fixing the transducer to the structure. The potential for simulation error through an oversimplification of the transduction problem is large. The present paper examines this issue by considering three standard approximation schemes with the view to assessing their effect on the accuracy of predictions of elastic wave scattering from a structural defect in an aircraft wing skin coupon.

1.1. Practical Context - Hot Spot Monitoring in a Wing Skin

The investigation is done in the context of a case study in SHM system design involving a complex substructure in the lower wing skin of the F-111C, a strike reconnaissance aircraft that was recently retired by the Royal Australian Air Force (RAAF). The region, shown in Figure 1, includes a main stiffener with a milled depression which is designed to allow fuel-flow between adjacent bays of the wing-box fuel tank. Cracks in the depression were detected in RAAF aircraft in the mid 1990's. At the time, these cracks posed a serious structural integrity problem, leading to a considerable amount of work by the RAAF and the Australian Defence Science and Technology Organisation on developing a cost-efficient solution. Ultimately, the issue was addressed in part by means of a Boron composite bonded repair (CBR) applied to the exterior of the wing skin [3].

A retrospective examination identified at least two opportunities where SHM might have produced substantial cost-savings in the management of this particular problem. The

two key opportunities were: (i) in assisting certification of the CBR, and (ii) in providing a lower-cost alternative to conventional NDI in monitoring the crack-prone region. The case also presented as a useful exemplar for the main technical impediments to a successful transition of piezoelectric methods of SHM to fleet use. The interested reader can refer to [1] for a broader discussion of the relevant issues. The current article takes a narrower perspective. It simply uses the geometric complexity of the wing-skin structure as a realistic test case for the evaluation of numerical simulation as a tool for SHM system design.

2. EXPERIMENTAL

A test coupon replicating the wing structure shown in Figure 1 was manufactured to allow for an experimental examination of the plate-wave dynamics in the stiffener depression. The measured dynamics serve as the comparative yardstick for the results of the numerical simulations described later. The coupon was milled from a plate of Al2024-T851, the same material used in the actual F-111 wing skin.

In a structure involving geometric complexity, the location of the acoustic source and receiver elements is an important factor in the detection sensitivity of an acousto-ultrasonic inspection system. The identification of optimal locations for transducer placement is therefore a critical design objective. As remarked previously, that objective is most efficiently addressed by numerical simulation. The present study considers only one part of that design objective - optimal placement of the receiver element. The source element was fixed to the wing skin structure at the location labelled **A** in Figure 1, which was determined on the basis of an engineering judgment about the acoustic power flow through the stiffener depression.

A simplification was also made in relation to the choice of scatterer, with a notch considered instead of a fatigue crack. The justification is that a notch has a regular geometry that can be modelled with good accuracy, affording a reliable basis for systematic comparison between model predictions and experimental observations of scattering. By contrast, the subsurface geometry of a crack is more complex and known with much less certainty, and the scattering characteristics of a crack are influenced by crack closure and other factors that are superfluous to the primary objective of the present study. The notch was semi-elliptical in profile, with a length of 30 mm, as measured at the surface of the depression, 1.85 mm in depth at its centre, and 0.8 mm wide.

A measurement of the plate wave dynamics in the coupon was made by scanning laser vibrometry applied on the external surface of the coupon. Only the out-of-plane component of the surface displacement was mapped and scans were taken at a spatial resolution of 1 mm, which is sufficient to resolve the dynamics in the panel at the frequency of interest. Scans taken prior to and following manufacture of the notch were used to separate the scattered field from the measured fields as follows,

$$u_s = u_n - u_b \tag{1}$$

where u is the measured displacement and the subscripts s, b and n define the scattered field, the incident field and the sum of these two fields respectively.

All of the results reported in this paper pertain to a piezoelectric drive frequency of 300 kHz, with the excitation supplied to the element as a Hanning modulated 5-cycle voltage tone-burst. The element was a Pz27 disc, 6.35 mm in diameter and 0.5 mm thick, and was adhesively bonded to the plate using a thin layer of silver-loaded epoxy.

3. NUMERICAL SIMULATION

A three-dimensional finite element model of the wing skin geometry was produced using the Femap pre/post-processor and solved in NEi Nastran. Linear tetrahedral elements were used in an unstructured mesh where the element side-dimension was constrained to a maximum size of 0.9 mm. The mesh surrounding the notch is shown in Figure 2. It was confirmed by means of the Rayleigh-Lamb dispersion relations that the mesh results in a sampling rate of 8.5 and 17.5 elements per wave length for the antisymmetric and symmetric modes respectively, satisfying guidelines for this type of modelling [4]. The solution was advanced using an explicit integration scheme at a time step of 0.1 μs, which meets the Courant-Freidrichs-Lewy condition for convergence.

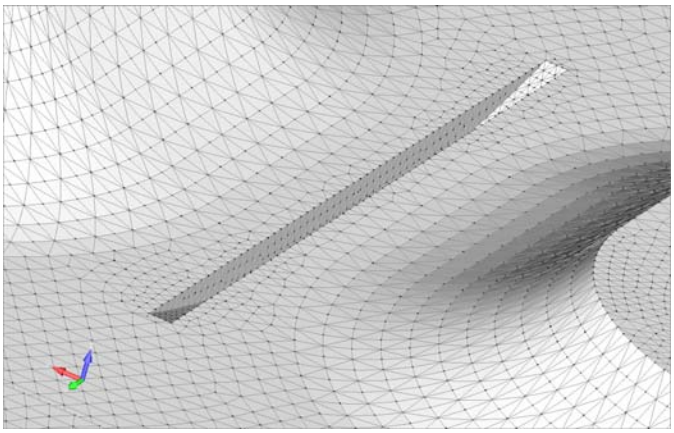

Figure 2. Mesh comprising tetrahedral elements surrounding the notch in the stiffener depression.

An accurate simulation of scattering requires an accurate description of the acoustic wavelength. A sensitivity study was done to map the variation in wavelength as a function of the ratio of the nominal wavelength to element size. The analysis revealed an error of less than 2.5% and 0.1% for the So and Ao modes respectively at the drive frequency of 300 kHz. Such an error was considered acceptable for the present exercise.

3.1. Piezoelectric Transducer Force Approximations

Figure 3 shows schematic illustrations of the three traction schemes considered in the simulations, in ascending order of sophistication. Starting from the left the first scheme is a normal point load, which represents a first approximation. The next case is a pressure loading over the transducer footprint [5] which is a natural extension of the point loading scheme, adding a length scale critical in describing the modal selectivity inherent in real transduction [6]. The third case involves shear traction, which includes the same length scale but intuitively provides a more satisfactory description of the forces applied by a surface-mounted element.

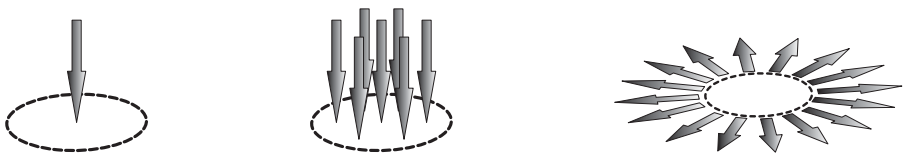

Figure 3. Schematic illustration of point (left), pressure (centre) and shear traction (right) loading schemes for a disc transducer.

Full piezoelectric coupling is also considered and serves as the nominal yardstick for the approximation schemes. Ultimately however, the predictive accuracy of all simulations is

assessed against experimental measurements of scattering in the coupon. The option of piezoelectric coupling was not available in the version of NASTRAN used in the present study so the case was dealt with in two steps. Firstly, COMSOL was used to develop the displacement field in a reduced structural geometry for a short simulation time, and these were then transferred to the corresponding nodes in the NASTRAN model. An adhesive bond was included in the transducer model. Unfortunately, the elastic properties of the adhesive could not be measured so representative values were derived from a published source [7]. A nominal bondline thickness of 50 μm was assumed.

4. RESULTS AND DISCUSSION

The scattered field was deduced from simulations involving the pristine and notched structures, largely mirroring the approach used in the experimental work. Comparisons were made in relation to a time-average of the displacement in the scattered field over an interval selected to ensure contributions were included from both incident symmetric as well as antisymmetric Lamb waves, i.e.,

$$u_a = \frac{1}{t_2 - t_1} \int_{t_1}^{t_2} |u_s| dt, \tag{2}$$

where t_1 and t_2 define the bounds of the time gate. The performance of the models in describing the modal composition of the elastic wave-field is examined first, using data obtained from the pristine structure. The velocity response along a short line running between and parallel to the main and secondary stiffeners was spectrally decomposed and compared to a theoretical prediction of the dispersion characteristics of the A_0 and S_0 modes corresponding to the panel thickness in that region. The results are shown in Figure 4.

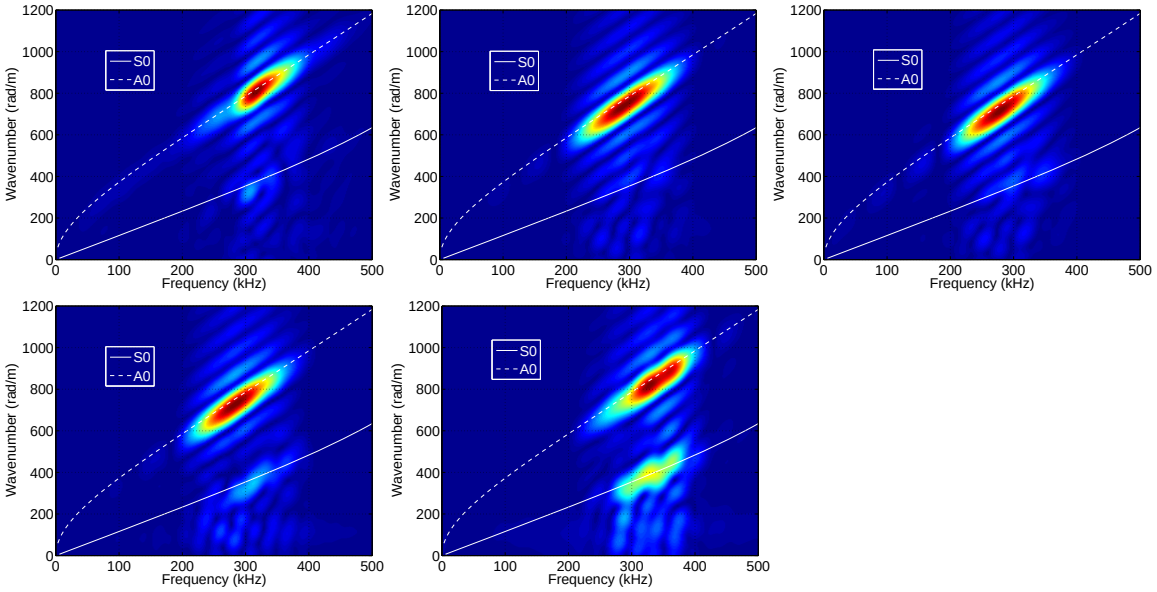

Figure 4. Comparison of computed and theoretical wavenumber spectra for experimental data (top left) and the four simulations: point load (top middle), pressure load (top right), shear traction (bottom left), and piezoelectric transduction (bottom middle).

Note that only the full piezoelectrically coupled simulation describes the upward shift in centre frequency witnessed in the experimental result. The absence of a shift is expected for the point load since the case omits a length scale, however the pressure and shear cases show no improvement over the point load and in fact are a little worse. A partial explanation is the effect of shear-lag in the adhesive layer bonding the transducer, which would tend to reduce the effective diameter of the transducer. No allowance for that was

made in the approximation scheme. Another interesting aspect of the comparison is that only the shear traction and full piezoelectric models produce a noticeable response in the S_0 mode, which the experimental result confirms is present although only weakly manifest in the out-of-plane displacement.

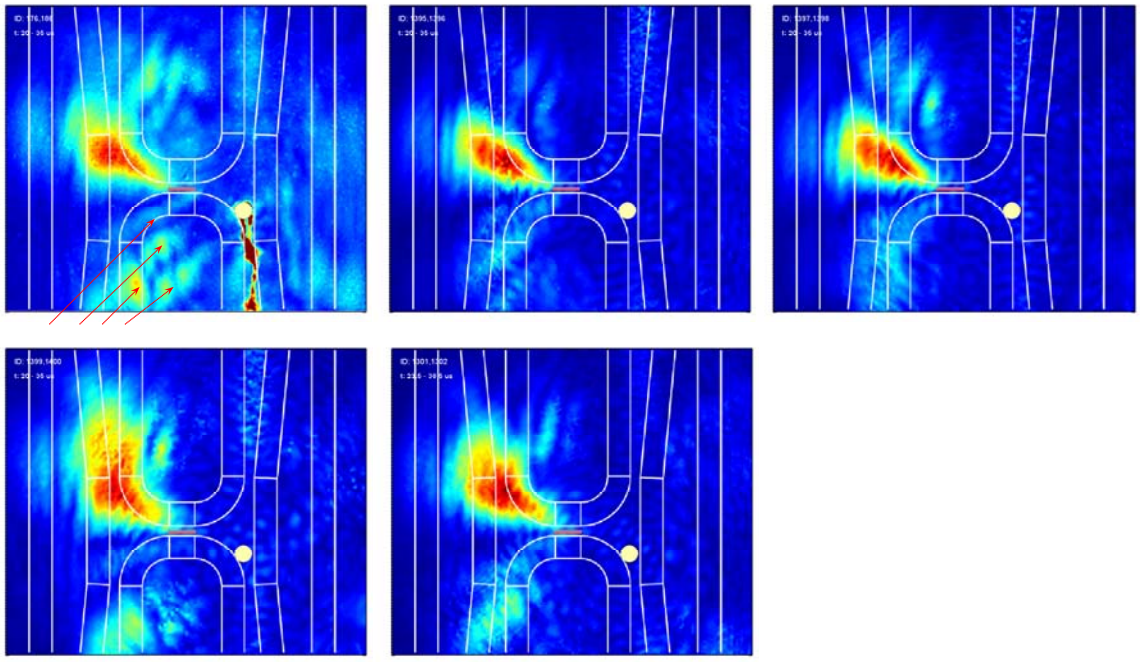

Figure 5. Distribution of u_a determined from experimental data (top left) and from simulations corresponding to a point load (top middle), pressure load (top right), shear traction (bottom left), and piezoelectric transduction (bottom middle).

Figure 5 compares scattered field predictions to the experimental result. The scattered field is strongest in the forward direction along a line bisecting the source and the notch, which is an intuitive result. The size, shape and orientation of the main feature is well described in all of the simulation results, illustrating that even a first approximation to the transduction process furnishes reasonable qualitative agreement. The more interesting and instructive comparisons are found in relation to finer detail in the scattered field, some of which is arrowed in the lower left quadrant of the measured result (top left sub-figure). Here, the differences between the simulations are significant with the shear traction case providing the most accurate description of the key features. Unexpectedly, the shear traction approximation outperforms the fully-coupled solution. The result implies a deficiency in the modelling of piezoelectric coupling, and illustrates that a multi-physics approach is also susceptible to error.

Figure 6 shows a quantitative comparison of the distribution of the normalised time-averaged displacement u_a along a line bisecting the main lobe of the scattered field in between the main and secondary stiffeners. Differences between the traces are most evident to the right of the peak which corresponds to the upper section of the main lobe in Figure 5. The coupled solution provides the best match to the experimental result, followed by the shear traction case. Note that the shear traction and coupled simulations predict a largely monotonic fall-off in displacement to the right of the peak (ignoring small-scale oscillations), at odds with the experimental trace which shows a reversal in that trend at approximately 45 mm. Interestingly, the point and pressure loading cases are more consistent with the experimental result in this region.

All of the simulations furnish potentially useful insight for system design. For instance, the location of peak scattering represents the position where a sensor would furnish the max-

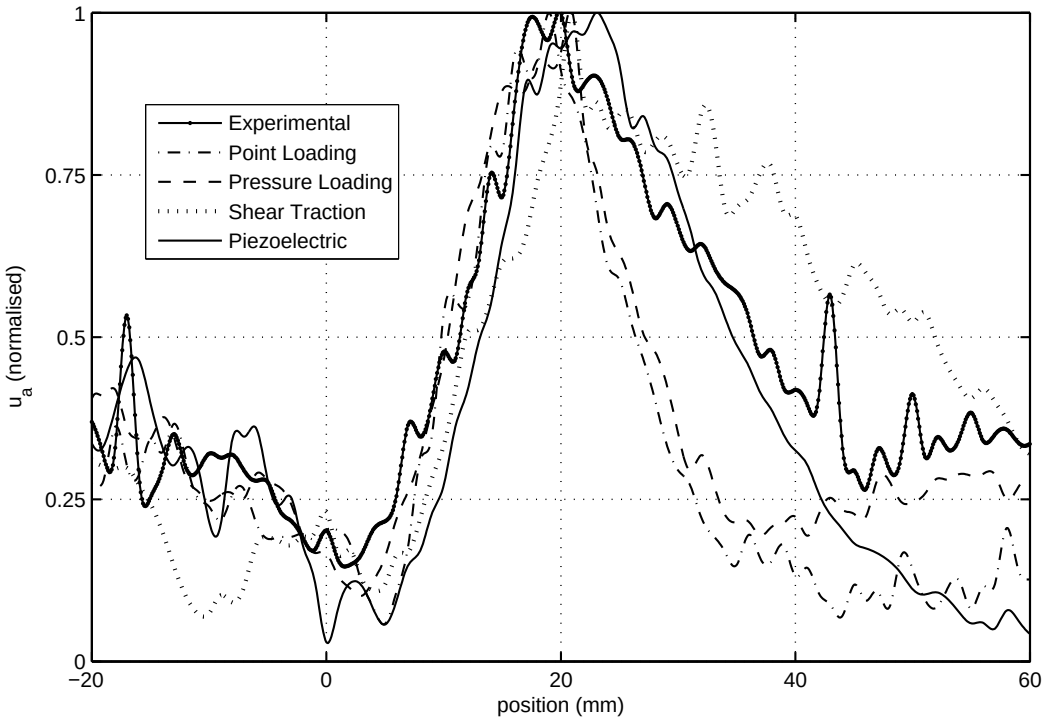

Figure 6. Distribution of the time-averaged displacement in the scattered field along a line bisecting the main lobe along a vertical line between the main and secondary stiffeners.

imum probability of detecting the scatterer. However, the design problem is unfortunately more complex and needs to consider a variety of other factors affecting sensor placement including the effect of operational loads on long-term transducer performance, access for installation and consideration of system powering and communication needs. Variations in the morphology, orientation, geometry, and severity of damage also need to be considered. This is especially important in terms of minimising diagnostic blind-spots across the broader spectrum of possible damage configurations. That design objective is potentially more important than, and not necessarily consistent with, maximising sensitivity to one particular damage configuration, as examined in the present work. When all of these various factors are added to a design problem the requirements on model fidelity increase substantially. Viewed in this context an accurate prediction of the location of peak scattering, while an encouraging result, is seen to provide only a limited measure of simulation performance.

The results of the present study suggest that an accurate description of the modal composition is essential for an accurate simulation of the propagation of guided waves through a complex structure and of the interaction of those waves with a structural defect. Figure 4 clearly illustrates that each scheme produces a slightly different mix of symmetric and antisymmetric mode in the elastic wave field. None of the simulations match the composition of the measured wave field exactly but the shear traction case does reasonably well, which probably explains why it also performs well in terms of the scattered field prediction. Significantly, the fact the dominant wavenumber in the simulated result differed noticeably from that in the measured field suggests scope for further improvement in the performance of this model, which might be achieved with an appropriate modification of the length scale to accommodate the shear-lag effect of the adhesive bondline.

The set of approximation schemes considered in the present article is by no means comprehensive. Other approaches are currently under investigation, including the PZT-force model proposed in [8] where transduction forces are determined from the piezoelectric constitutive relations. The results of this expanded study will be reported elsewhere.

5. CONCLUSIONS

This paper reports on an investigation into the accuracy of numerical finite element simulations of elastic wave scattering from a structural defect in a metallic wing skin component. A key objective of the study was to determine the effect on simulation accuracy of various force-based approximations to piezoelectric transduction, with a view to justifying that approach as a means of reducing the computational burden involved in solving acousto-ultrasonic modelling problems. On the basis of comparison to experimental observations of scattering in a representative wing-skin coupon it was found that approximation schemes are capable of furnishing a predictive accuracy approaching that of fully coupled simulations. Interestingly, it was shown that shear-traction loading produced a better qualitative description of some aspects of the scattered field than the coupled simulation, which was thought to stem from uncertainties in the material properties of the piezoelectric source and possibly also of the adhesive bondline. The result underscores the need for care in applying a fully coupled approach, as well as the need more generally for experimental verification of simulation results, regardless of how transduction is modelled.

REFERENCES

1. N. Rajic. *Development of an active smart patch for aircraft repair.* Encyclopedia of Structural Health Monitoring - Chapter 107. John Wiley and Sons Limited, Chichester, U.K., 2009.
2. N. Rajic. A numerical model for the piezoelectric transduction of stress waves. *Smart Materials and Structures*, 15:2262–1164, 2006.
3. A. Baker, N. Rajic, and C. Davis. Towards a practical structural health monitoring technology for patched cracks in aircraft structure. *Composites Part A: Applied Science and Manufacturing*, 40(9):1340 – 1352, 2009.
4. D.N. Alleyne and P. Cawley. The interaction of lamb waves with defects. *Ultrasonics, Ferroelectrics and Frequency Control, IEEE Transactions on*, 39(3):381 –397, May 1992.
5. L. Tierang, M. Veidt, and S. Kitipornchai. Modelling the input-output behaviour of piezoelectric structural health monitoring systems for composite plates. *Smart Materials and Structures*, 12(5):836, 2003.
6. V. Giurgiutiu. Tuned lamb wave excitation and detection with piezoelectric wafer active sensors for structural health monitoring. *Journal of Intelligent Material Systems and Structures*, 16(4):291–305, 2005.
7. http://www.matweb.com, 2012.
8. J.H. Nienwenhuis, Jr. Neumann, J.J., D.W. Greve, and I.J. Oppenheim. Generation and detection of guided waves using pzt wafer transducers. *Ultrasonics, Ferroelectrics and Frequency Control, IEEE Transactions on*, 52(11):2103 –2111, Nov. 2005.